



estimated to average 1 hour per response, including the time for reviewing instructions, searching existing data sources, gathering and reviewing the collection of information. Send comments regarding this burden estimate or any other aspect of this collection of information, including suggestions for reducing this burden, to Washington Headquarters Services, Directorate for Information Operations and Reports, 1215 Jefferson Avenue, Washington, DC 20540, and to the Office of Management and Budget, Paperwork Reduction Project (0704-0188), Washington, DC 20503.

REPORT DATE May 14, 1993		3. REPORT TYPE AND DATES COVERED Final Report Oct. 1, 1989-Dec. 31, 1992	
4. TITLE AND SUBTITLE An Investigation of the Role of Second Phase Particles in the Design of Ultra High Strength Steels of Improved Toughness		5. FUNDING NUMBERS DAA03-89-K-0175	
6. AUTHOR(S) Warren M. Garrison, Jr.		8. PERFORMING ORGANIZATION REPORT NUMBER	
7. PERFORMING ORGANIZATION NAME(S) AND ADDRESS(ES) Dept. of Materials Science and Engineering Carnegie Mellon University Pittsburgh, PA 15213		9. SPONSORING/MONITORING AGENCY NAME(S) AND ADDRESS(ES) U. S. Army Research Office P. O. Box 12211 Research Triangle Park, NC 27709-2211	
11. SUPPLEMENTARY NOTES The view, opinions and/or findings contained in this report are those of the author(s) and should not be construed as an official Department of the Army position, policy, or decision, unless so designated by other documentation.		10. SPONSORING/MONITORING AGENCY REPORT NUMBER ARO 27407.1-MS	
12a. DISTRIBUTION/AVAILABILITY STATEMENT Approved for public release; distribution unlimited.		12b. DISTRIBUTION CODE 93-15449	
13. ABSTRACT (Maximum 200 words) The influence of inclusion distributions and fine scale microstructure on the fracture toughness and fracture processes of ultra high strength steels have been investigated. The inclusion distributions vary in the sulfide type and the sulfide types considered were MnS, CrS, La ₂ O ₂ S and Ti ₂ CS. The MnS and CrS particles are smaller and more closely spaced than particles of La ₂ O ₂ S. Resistance to void nucleation is the same if the sulfur is gettered as CrS, MnS or La ₂ O ₂ S. The particles of Ti ₂ CS are smaller and much more resistant to void nucleation than the other sulfide types. The fine scale microstructures were those obtained for the as-quenched, tempered at 425°C and tempered at 510°C conditions for HY180 and AF1410 steels. The topics then addressed are (a) effect of fine scale microstructure and inclusion distributions on blunting behavior, (b) the role of inclusion spacing at constant inclusion volume fraction on fracture toughness of three fine scale microstructures for HY180 steel, (c) effect of gettering sulfur as Ti ₂ CS on the fracture toughness of three fine scale microstructures of HY180 steel, (d) morphology of Ti ₂ CS particles, (e) effect of gettering sulfur as Ti ₂ CS on the fracture toughness of AF1410 steel tempered at 510°C, and (f) conclusions regarding improving toughness by gettering sulfur as Ti ₂ CS.			
14. SUBJECT TERMS steels, fracture toughness, inclusions, void nucleation, titanium carbosulfides		15. NUMBER OF PAGES 33 pages	
17. SECURITY CLASSIFICATION OF REPORT UNCLASSIFIED		16. PRICE CODE	
18. SECURITY CLASSIFICATION UNCLASSIFIED		20. LIMITATION OF ABSTRACT UL	
19. SECURITY CLASSIFICATION OF ABSTRACT UNCLASSIFIED			

DTIC
SELECTED
JUL 12 1993

93-15449
34pt

**An Investigation of the Role of
Second Phase Particles in the Design
of Ultra High Strength Steels
of Improved Toughness**

Final Report

U.S. ARMY RESEARCH OFFICE

GRANT NUMBER: DAAL03-89-K-0175

Period: October 1, 1989 thru December 31, 1992

**Attention: Dr. W. Simmons
Metallurgy and Materials Science Division
U.S.Army Research Office
Triangle Park, NC 27709**

DTIC QUALITY INSPECTED 5

**W. M. Garrison, Jr.
Department of Materials Science and Engineering
Carnegie Mellon University
Pittsburgh, PA 15213**

Accession For	
NTIS CRA&I	<input checked="" type="checkbox"/>
DTIC TAB	<input type="checkbox"/>
Unannounced	<input type="checkbox"/>
Justification	
By	
Distribution /	
Availability Codes	
Dist	Avail and/or Special
A-1	

Table of Contents

1.	Introduction	3
2.	Fracture Toughness and Ductile Fracture	4
3.	Approach: Microstructure and Fracture Toughness	4
3.1	Inclusion Distributions	5
3.2	Fine Scale Microstructure	5
3.3	Fracture Processes	5
4.	Summary of Results	6
4.1.	Steels selected for study	6
4.2.	Effects of fine scale microstructure and inclusion distributions on blunting behavior	7
4.3.	Effects of inclusion spacing on toughness	7
4.4.	Effect on toughness of making sulfides more resistant to void nucleation (Ti_2CS)	10
4.5.	Conclusions	13
5.	Students	14
6.	Patents	14
7.	Commercial Applications	14
8.	References	15
9.	Tables	16
10.	Figures	24.

1. Introduction

When ultra high strength steels fracture by the growth and coalescence of voids nucleated at second phase particles, the voids are usually nucleated first at inclusions which are normally sulfide and oxide particles. One can consider the microstructure of steels to consist of inclusions distributed through a fine scale microstructure which is largely defined by composition and heat treatment. The fine scale microstructure has some inherent toughness, and inclusions incorporated in the microstructure result in a toughness less than this inherent toughness. A fundamental goal of past work has been to investigate how inclusion distributions can be best controlled in order to minimize their effect on toughness and to allow the material to achieve toughnesses as close to the inherent toughness of the fine scale microstructure as possible.

The approach taken to minimizing the detrimental effect of inclusions on toughness has been to

1. Develop methods of producing inclusion distributions which vary in inclusion spacing, volume fraction and resistance to void nucleation.
2. Investigate how changing inclusion distributions influences fracture toughness as a function of fine scale microstructure.
3. Develop from these experiments and studies of the fracture process an understanding of how variables used to characterize inclusion distributions and fine scale microstructures combine to determine fracture toughness.

The work done over the past three years relevant on improving toughness by controlling inclusion distributions is summarized. This work has focused on the effect of fine scale microstructure and inclusion distributions on blunting behavior, the effects of inclusion spacing at constant inclusion volume fraction and fixed fine scale microstructure on toughness, and the effect of making inclusions more resistant to void nucleation on toughness as a function of fine scale microstructure.

One important result of this work is that for many fine scale microstructures an effective approach to minimizing the detrimental effect of inclusions on toughness has been to get sulfur as particles of Ti_2CS rather than as particles of MnS , CrS or La_2O_2S . The degree to which toughness can be improved by getting sulfur as Ti_2CS is illustrated in Fig. 1 for HY180 [1] and AF1410 [2] steels. The improvements in fracture toughness realized by getting sulfur as Ti_2CS is attributed to the Ti_2CS particles being more resistant to void nucleation than particles of other sulfide types [1].

2. Fracture Toughness, Microstructure and Ductile Fracture

Three measures of fracture initiation toughness are the plane strain fracture toughness, K_{IC} [3], the crack tip opening displacement (δ) at fracture (δ_{IC}) [4] and the J-integral at fracture (J_{IC}) [5]. The three parameters are related:

$$\delta_{IC} = d_n \frac{J_{IC}}{\sigma_0} \quad \sigma_0 = (\sigma_{YS} + U.T.S) / 2 \quad (1a)$$

$$J_{IC} = \frac{K_{IC}^2}{E'} \quad E' = E \text{ for plane stress} \quad (1b)$$

$$= E/(1-\nu^2) \text{ for plane strain}$$

where E is Young's modulus, ν is Poisson's ratio and d_n is a function of the yield strain, the work hardening exponent n and whether plane stress or plane strain conditions are encountered [6]; typically d_n is about 0.5.

The toughness of a steel is determined not only by the volume fraction [7], spacing [2,8] and void nucleation characteristics [1,9] of the inclusions but other microstructural features as well. In our studies of fracture initiation, when fracture is by the coalescence of voids nucleated at second phase particles, the following microstructural definitions have been adopted. Here, microstructure is separated into two categories: primary particles and fine scale microstructure. The primary particles are the particles which first nucleate voids during the fracture process; in steels the primary particles are typically sulfides and oxides. The fine scale microstructure is everything except the the primary particles and consists of the secondary particles and other microstructural features. Secondary particles are particles which nucleate voids late (if at all) in the fracture process. They can directly influence the fracture process if they nucleate voids and can indirectly influence the fracture process by either influencing grain size (carbides/nitrides inherited from the austenitizing temperature in steels) or by influencing the flow properties if present at sufficiently high volume fractions, as is typically achieved when particles are precipitated during tempering. Other microstructural features of possible importance in the fracture process include grain size and dislocation density and structure. These microstructural features can influence toughness and they appear to do so in a highly complex way. For example, primary particles can influence toughness through their spacing, but the effects of primary particle spacing may depend critically on the grain size of the material.

3. Approach: Microstructure and Fracture Toughness

As fracture initiation toughness is influenced by both the inclusion distributions and the fine scale microstructure, the goal has been to systematically vary inclusion particle spacing, void nucleation resistance of inclusions and fine scale microstructure, and to

investigate how these variations influence toughness and the fracture process. This has been done in the following ways.

3.1. Quantifying and Varying Inclusion Distributions

Quantifying the inclusion distributions has involved determining their volume fraction, average radius, average three-dimensional nearest neighbor spacing and their void nucleation and growth characteristics as reflected in void volume fraction (normalized by initial inclusion volume fraction) as a function of strain in uniaxial tension.

The inclusion distributions have been varied by gettering the sulfur as either MnS, CrS, La₂O₂S or Ti₂CS. When the sulfur is gettered as MnS or CrS the inclusion size and spacing are small and void generation from inclusions is the same, whether the sulfides are CrS or MnS [2,10]. Gettering sulfur as La₂O₂S results in larger, more widely spaced inclusions [2] but these inclusion distributions behave similarly in terms of void generation to the inclusion distributions obtained when sulfur is gettered as MnS or CrS [11]. By adding small amounts of titanium the sulfur is gettered as small particles of Ti₂CS and this results in an inclusion distribution much more resistant to void nucleation than the inclusion distributions in which sulfur is gettered as MnS, CrS or La₂O₂S [10].

3.2. Quantifying Fine Scale Microstructures

The fine scale microstructure has been typically quantified by determining prior austenite grain size, the type, volume fraction and size distribution of secondary particles, and by measuring the plane strain tensile ductility (Fig. 2) in addition to the usual smooth axisymmetric tensile properties.

The plane strain tensile ductility has been emphasized in this work for two reasons. First, at least at high strength levels, the plane strain tensile ductility depends only on the fine scale microstructure and is a measure of the inherent ductility, the ductility of the fine scale microstructure if all inclusions were removed from the microstructure [12]. Second, the strain state is similar to that expected at the crack tip. Thus, the plane strain tensile ductility would appear to be a measure of the inherent ductility of the fine scale microstructure appropriate to fracture initiation.

3.3. Studying Fracture Processes

The fracture process has been examined by cross-sectioning J_{IC} specimens strained to different J levels but not fractured; this work led to the conclusion that blunting to vertices, not smooth blunting, is exhibited by many microstructures and that blunting behavior has enormous consequences in terms of fracture initiation toughness and it would be inappropriate to compare results for different materials unless the blunting behaviors are known [13,14]. Finally, SEM micrographs and extraction replicas of fracture surfaces

examined in TEM have been used to determine the inclusions and secondary particles actually involved in the fracture process.

4. Summary of Results

In this section work carried out for the past three years on investigating microstructural effects on toughness and the fracture process are summarized. First the steels that were selected for study will be described. The topics then addressed are (a) effect of fine scale microstructure and inclusion distributions on blunting behavior, (b) the role of inclusion spacing at constant inclusion volume fraction on fracture toughness of three fine scale microstructures for HY180 steel, (c) effect of getting sulfur as Ti_2CS on the fracture toughness of three fine scale microstructures of HY180 steel, (d) morphology of Ti_2CS particles, (e) effect of getting sulfur as Ti_2CS on the fracture toughness of AF1410 steel tempered at $510^\circ C$, and (f) conclusions regarding improving toughness by getting sulfur as Ti_2CS .

4.1. Steels Selected for Study

The two steels selected for study were HY180 and AF1410. HY180 was selected because it was in an old commercial heat of HY180 steel that the benefits of getting sulfur as Ti_2CS was first observed and it was preferred to not change materials [15]. AF1410 was used because it has a higher yield strength than HY180, but is very similar in terms of composition and microstructure.

HY180 steel has a nominal composition (in wt.%) of 0.10C/10Ni/8Co/2Cr/1Mo and AF1410 has a nominal composition (in wt.%) of 0.16C/10Ni/14Co/2Cr/1Mo. Both steels are austenitized, quenched to room temperature and then tempered. In the as-quenched condition both steels have a lath martensite structure with interlath films of retained austenite; on tempering at $425^\circ C$ only Fe_3C is observed to precipitate within the laths for both steels, while, after tempering at $510^\circ C$, only fine needles of $(Mo,Cr)_2C$ are precipitated within the laths [16,17]. Typical behavior as a function of tempering temperature is depicted in Fig. 3 for HY180 and AF1410. The fracture behavior for these two steels has typically been assessed for the as-quenched microstructure, the tempered at $425^\circ C$ and the tempered at $510^\circ C$ microstructures for three different inclusion distributions based on getting sulfur as MnS, La_2O_2S or Ti_2CS . The as-quenched microstructure was used because smooth blunting had been observed only for as-quenched microstructures. The $425^\circ C$ microstructure was used because it has the minimum toughness and the $510^\circ C$ microstructure was used because this structure has the optimum combination of strength and toughness.

4.2. Effects of Fine Scale Microstructure and Inclusion Distributions on Blunting Behavior

McClintock [18] pointed out that the initially sharp fatigue crack introduced in specimens used to measure K_{IC} and J_{IC} could, in principle, blunt to a variety of shapes, including two and three corner (vertices) geometries and the smooth, semi-circular shape normally assumed; these blunting geometries are illustrated in Fig. 4. McMeeking, [19,20] on the basis of calculations of the growth of voids directly ahead of the crack tip, suggested blunting to vertices might be associated with higher toughness than smooth blunting.

Cross sections of strained but not fractured compact tension J_{IC} specimens have been examined for a number of fine scale microstructures containing different inclusion distributions. Blunting behavior does not appear to be influenced by changes in inclusion distributions and thus appears to be determined only by the fine scale microstructure; smooth blunting has been observed only when the work hardening exponent is high ($n \geq 0.16$) [13,14]. The effects of fine-scale microstructure on toughness are summarized in Fig. 5. For fixed inclusion volume fraction and spacing (in Fig. 5 only small inclusion spacings are considered), toughness increases rapidly with plane strain ductility for a given blunting behavior. In addition, the data suggest that for a given inclusion distribution and given level of constrained ductility, microstructures which blunt to vertices can have considerably higher toughnesses than microstructures which blunt smoothly.

The three conditions examined for HY180 and AF1410, the as-quenched, tempered at 425°C, and tempered at 510°C microstructures, blunted to vertices and this blunting behavior was not influenced by changing inclusion distributions. Surprisingly, even the as-quenched microstructures blunted to vertices, even though the as-quenched work hardening exponents ($n = 0.11$) were higher than for the tempered at 425°C and 510°C microstructures [10].

4.3. Effect of Inclusion Spacing on Toughness

Here three topics are considered. First are summarized the results of experiments in which the inclusion spacing is varied at constant inclusion volume fraction for three microstructures of HY180 steel. Second, results are summarized which indicate grain size has a very potent effect on toughness when the inclusions are small and closely spaced, but not when they are large and widely spaced. In addition, the possibly critical role of oxides when the sulfur is gettered as Ti_2CS is discussed.

4.3.a. Effect of Inclusion Spacing on Toughness at Constant Inclusion Volume Fraction and Fixed Fine Scale Microstructure

Rice and Johnson [8], considering a void of radius R_0 a distance X_0 ahead of a smoothly blunting crack tip obtained the result $\delta_{IC} = X_0 F(X_0/R_0)$, where $F(X_0/R_0)$

increases slowly with increasing X_0/R_0 . This result is usually applied by regarding X_0 as the three dimensional nearest neighbor inclusion spacing and taking $X_0/R_0 = 0.89f^{-1/3}$ where R_0 is the average inclusion radius and f is the inclusion volume fraction. This approach predicts $\delta_{IC} = X_0F(f)$ and that at fixed volume fraction δ_{IC} will increase linearly with increasing X_0 and that $\delta_{IC}/X_0 = F(f)$ where for relatively clean materials $F(f) \cong 2$. Previous results were not consistent with those predictions.

Previous results are shown in Fig. 6 where δ_{IC} is plotted as a function of X_0 at constant f for AF1410 steel aged at 425°C and 510°C where the small spacings are associated with CrS and the two larger spacings are obtained by getting the sulfur as La_2O_2S . First, δ_{IC} tends to increase with X_0 and then appears to approach some limiting value as X_0 increases. Thus, once X_0 exceeds some characteristic value, it appears δ_{IC} becomes independent of X_0 . These microstructures blunt to vertices and we have no similar data for microstructures which blunt smoothly, but suspect similar behavior would be observed. Second, as shown in Table 1, values of δ_{IC}/X_0 are much larger than predicted for Rice and Johnson even for small particle spacings; for smooth blunting these values are as high as 18 compared to the result of about 2 predicted by Rice and Johnson, which is often regarded to be an upper bound.

The effect of inclusion spacing at constant inclusion volume fraction on toughness has been explored as a function of fine scale microstructure for HY180 steel [10]. The goals were (a) to determine the effect of inclusion spacing on toughness, (b) to determine if getting sulfur as La_2O_2S was as effective in improving the toughness of HY180 as it was in improving the toughness of AF1410.

The compositions, inclusion characteristics, carbides inherited from the austenitizing temperature and prior austenite grain sizes and mechanical properties of the two heats are summarized in Tables 2, 3, 4 and 5 respectively. Heat 1 contains MnS and heat 2 contains La_2O_2S . As shown in Table 3 the La modified heat has $X_0 = 7.5 \mu\text{m}$ compared to $2.4 \mu\text{m}$ for the MnS heat.

The data show that the lanthanum modified heat has better toughness than heat 1 (MnS) for the three microstructures considered. Based on previous work it was anticipated this improvement in toughness is due to the increased inclusion spacing. The void nucleation results indicate that the inclusions in the lanthanum modified heat are not more resistant to void nucleation than the inclusions in the MnS sulfide heat (Fig. 7b). In addition, the two heats have almost the same prior austenite grain sizes and very similar dispersions of carbides inherited from the austenitizing temperature in terms of types, sizes and volume fractions (Table 4). Also, the two heats have almost the same plane strain tensile ductility and work hardening exponent for the as-quenched microstructure; this is

also the case for the tempered at 425°C microstructure. Finally, while the inclusion volume fraction appears smaller for heat 1 than for heat 2, the improvements in toughness cannot be attributed to differences in inclusion volume fraction, as the dependence of δ_{1C} on inclusion volume fraction, f , is fairly weak and δ_{1C} scales as $f^{-1/3}$. Therefore it seems reasonable to conclude for these two microstructures that the improvements in toughness associated with the lanthanum additions are due to the increase in inclusion spacing. However, this conclusion is more difficult to make for the tempered at 510°C microstructure. The plane strain tensile ductility is about the same for heat 1 (MnS) and heat 2 (La₂O₂S) for the as-quenched microstructure and after tempering at 425°C, but not after tempering at 510°C. On tempering at 510°C the plane strain tensile ductility of heat 2 (La₂O₂S) is much higher than expected; a value of 0.36 to 0.37 would have been expected, but a value of 0.44 was obtained. If this rather high value is correct, then, given that our results indicate (everything else being equal) that toughness increases rapidly with increasing plane strain tensile ductility, it would not be appropriate to conclude the improved toughness of the lanthanum modified heat tempered at 510°C is due primarily to the increase in inclusion spacing.

The results indicate that gettering sulfur as La₂O₂S results in better toughness than when the sulfur is gettered as MnS. Moreover, while the improvement in toughness can be attributed to increased inclusion spacing for the as-quenched and tempered at 425°C microstructures, the toughness does not increase linearly with X_0 .

4.3.b. Grain Size Effects

Based on studies of the effects of austenitizing temperature it was hypothesized that grain size would have a significant effect on toughness for only small inclusion spacings. This hypothesis has been tested by utilizing three heats of a 0.07C/9Ni steel, two heats containing MnS and one heat containing La₂O₂S [21]. The compositions and inclusion characteristics of the three heats are summarized in Tables 6 and 7 respectively. As shown in Fig. 8 the Charpy impact energies of the MnS heats are remarkably sensitive to grain size, while the Charpy impact energy of the La modified heat containing large, widely spaced inclusions is not. As the Ti₂CS inclusions to be discussed are typically quite small, grain size should be important in achieving the maximum toughness for steels in which sulfur is gettered as Ti₂CS.

4.3.c. Role of Oxide Volume Fraction and Spacing on Toughness

As the oxides in these HY180 heats appear no more resistant to void nucleation than MnS [11], it seems reasonable, from the standpoint of fracture, to consider the sulfides and oxides as one particle distribution. However, when the sulfides are Ti₂CS the sulfides and oxides are very different from the standpoint of void nucleation and the oxides

should be the "weak link" in the fracture process. The effect of particle spacing on toughness suggests that if the oxides are small and closely spaced then the oxides, even if present at small volume fraction, could dominate the fracture process even if the sulfur is gettered as Ti_2CS . Therefore, to take full advantage of gettering the sulfur as Ti_2CS it is necessary to achieve widely spaced oxides at a low volume fraction.

4.4. Effect of Making Sulfides More Resistant to Void Nucleation

The goals of this work were to investigate conditions required to getter sulfur as Ti_2CS and the effects of gettering sulfur as Ti_2CS on fracture toughness as a function of fine scale microstructure at constant strength level and as a function of the strength of the fine scale microstructure[1,10].

4.4.a. Effect of Gettering Sulfur as Ti_2CS on the Toughness of HY180 Steel

Two heats of HY180 steel, referred to here as heat 3 and heat 4, were melted without deliberate additions of manganese or of lanthanum, but with additions of 0.02 and 0.012 wt.% titanium respectively. The compositions of these heats are given in Table 2. The inclusion characteristics are listed in Table 3 and prior austenite grain sizes and the types, volume fractions and average sizes of the carbides inherited from the austenitizing temperature are given in Table 4.

The mechanical properties of these heats are compared to those of the heats containing MnS (heat 1) and La_2O_2S (heat 2) for the as-quenched condition and after tempering at 425°C and 510°C in Table 5. For all three microstructure the toughnesses are significantly higher when the sulfur is gettered as Ti_2CS . The improvements in toughness associated with gettering the sulfur as Ti_2CS are most dramatic for the tempered at 510°C microstructure; for this microstructure the 0.02 wt.% Ti and 0.012 wt.% Ti heats have fracture toughnesses of $480 \text{ MPa}\sqrt{\text{m}}$ and $550 \text{ MPa}\sqrt{\text{m}}$ respectively, compared to fracture toughnesses of $267 \text{ MPa}\sqrt{\text{m}}$ and $339 \text{ MPa}\sqrt{\text{m}}$ for the MnS and La_2O_2S heats respectively.

The conclusions drawn from the microstructural data and the mechanical property results are the following.

4.4.a.1. The sulfides in heats 3 and 4 are Ti_2CS : Based on both chemical analysis using windowless energy dispersive spectrometry of particles in aluminum extraction replicas and electron diffraction patterns, the sulfides are Ti_2CS .

4.4.a.2. Titanium additions alter the type, size and volume fraction of the carbides inherited from the austenitizing temperature: The titanium additions not only alter the sulfide type, but are also associated with a smaller grain size, a change in the types of carbides inherited from the austenitizing temperature, a reduction in the size of these carbides, and, at the higher titanium level, an increase in the volume fraction of these

carbides (Table 4). Because of these changes in carbide type from $M_{23}C_6$ and M_2C to MC and M_2C , as well as refinement in carbide size and grain size, the plane strain tensile ductility of the 0.02 wt.% titanium heat is the same as that of the MnS heat, even though the carbide volume fraction of the 0.02 wt.% titanium heat is higher than the carbide volume fraction of the MnS heat, and the plane strain tensile ductility of the 0.012 wt.% titanium heat is higher than that of the MnS heat.

4.4.a.3. Titanium additions only slightly modify oxide dispersions: The oxides in heats 3 and 4 are not substantially different from the oxides in the MnS heat (heat 1). The oxides in these three heats have an average radius of about $0.5 \mu\text{m}$ and contain Mg, Al and Ti, where the relative amounts of these elements vary from particle to particle; the oxides in the titanium modified heats tend to contain more titanium than the oxides in the MnS heat.

4.4.a.4. The improved toughnesses associated with getting the sulfur as Ti_2CS is due to the improved resistance of these particles to void nucleation: The improved toughness of the titanium modified heats is attributed to the Ti_2CS particles being more resistant to void nucleation than particles of the other sulfide types. This is most easily demonstrated by comparing heat 1 (MnS) and heat 3 (0.02 wt.% Ti). For a given tempering condition these two heats have similar strength levels, work hardening behavior and plane strain tensile ductility. The inclusion volume fractions are very similar in both heats. Therefore, the critical difference between the two heats is the improved resistance to void nucleation of the particles in the Ti_2CS heat; this improved resistance to void nucleation is demonstrated in Figs. 7a and 7b for the as-quenched and tempered at 510°C microstructures respectively.

4.4.a.5. Getting sulfur as Ti_2CS is most effective after tempering at 510°C : While the heats in which the sulfur is gettered as Ti_2CS have the highest toughness for all three microstructures, getting the sulfur as Ti_2CS is most effective after tempering at 510°C . The ratio $\delta_{IC}(Ti_2CS; 0.02 \text{ wt.\%Ti})/\delta_{IC}(La_2O_2S)$ is 1.89 after tempering at 510°C , 1.28 for the as-quenched microstructure and 1.66 after tempering at 425°C . These differences may be due to differences in void nucleation at the Ti_2CS particles. The void generation results in Fig. 7c suggest voids are nucleated at the Ti_2CS particles at lower strains in the as-quenched structure than in the tempered at 510°C microstructure. Possibly the lower void nucleation strain for the as-quenched microstructure is due to the higher work hardening capacity of the as-quenched microstructure.

4.4.a.6. When sulfur is gettered as Ti_2CS titanium additions of 0.01 wt% or less should be used: The 0.012 wt.% titanium typically has a higher plane strain ductility than the 0.02 wt.% titanium heat, apparently because the volume fraction of

carbides inherited from the austenitizing temperature is higher for the 0.02 wt.% titanium heat than for the 0.012 wt.% titanium heat. As the results in Fig. 5 imply a strong effect of plane strain ductility on toughness, it is believed the titanium additions should be 0.01 wt% and possibly less.

4.4.a.7. Role of oxides in determining toughness of titanium modified steels: Fracture surfaces of heat 1 (MnS) and heat 3 (0.02 wt.% Ti) are shown in Fig. 9. Oxides are visible in the larger voids on fracture surfaces of heat 3 (0.02 wt.% Ti) and are involved in the fracture process in the heats containing Ti_2CS ; it is believed the excellent toughnesses of these heats are due in part to their low oxygen levels and the relatively large spacing of oxide particles.

4.4.b. Morphologies of Ti_2CS Particles

The Ti_2CS particles in our experimental Ti_2CS heats were typically thin plates, although the sizes varied. Only the larger plates could be seen on fracture surfaces using the scanning electron microscope and, as shown in Fig. 10a, these particles had typically fractured. Based on observations of extraction replicas about 20% of the Ti_2CS particles on the fracture surface were these large fractured plates. Also seen on these extraction replicas were Ti_2CS particles which had not fractured, and the sizes of these particles ranged from that shown in Fig. 10b to diameters in the plane of the plates as small as 500Å.

4.4.c. Extension to Higher Strength Levels Using AF1410 Steel

As discussed earlier, the steel selected to test the extent to which gettering sulfur as Ti_2CS improved toughness at high strength levels was AF1410. In Tables 8 and 9 are compared the respective chemistries and the mechanical properties of heats of AF1410 steel in which the sulfur is gettered as MnS (heat A1), CrS (heat A2), La_2O_2S (heat A3) and Ti_2CS (heat A4) [10,22]. Again the inclusions in the heats containing MnS and CrS are much smaller than the heats containing the La_2O_2S and they have lower toughness than the La_2O_2S heat. The Ti_2CS particles in heat A4, as was the case for HY180 steel, form as plates and are typically quite small, although large fractured plates are commonly observed on the fracture surface. The fracture toughness of the Ti_2CS heat of AF1410 was 341 MPa \sqrt{m} compared to 199 MPa \sqrt{m} for the La_2O_2S heat.

The toughness of AF1410 steel is strongly dependent on prior austenite grain size when the sulfur is gettered as Ti_2CS . When the final austenitizing temperature is increased from 823°C to 1000°C the Charpy impact toughness of AF1410 tempered at 510°C actually increases when the sulfur is gettered as La_2O_2S , but decreases by a factor of two when the sulfur is gettered as Ti_2CS [22].

The temperature at which Ti_2CS dissolves in AF1410 steel is about $1250^{\circ}C$. This suggests the Ti_2CS particles are very stable and will precipitate from the austenite at high temperatures, even at the low titanium content of this alloy (heatA4).

4.5. Conclusions

4.5.a Conclusions Regarding the Effect of Gettering Sulfur as Ti_2CS on the Toughness of Ultra High Strength Steels

About the effect of gettering sulfur as Ti_2CS on the fracture toughness of ultra high strength steels the following conclusions seem justified at this point:

1. Gettering sulfur as Ti_2CS is much more effective in improving toughness than gettering sulfur as MnS or La_2O_2S
2. Improvements in toughness due to gettering sulfur as Ti_2CS are primarily due to the particles of Ti_2CS being more resistant to void nucleation than particles of MnS or La_2O_2S .
3. The degree to which gettering sulfur as Ti_2CS improves toughness can depend on the fine scale microstructure, even at relatively constant strength levels.
4. The titanium content of 0.012 wt.% which was sufficient to getter the sulfur as Ti_2CS in the alloys investigated also alters the type and size of the carbides inherited from the austenitizing temperature. These changes in carbides result in improved plane strain ductility, which also helps promote increased toughness.
5. The amount of the titanium addition can influence the volume fraction of carbides inherited from the austenitizing temperatures. Titanium additions of 0.02 wt.% resulted in more undissolved carbides than 0.012 wt.% titanium.
6. Oxides in the MnS and Ti_2CS heats of HY180 and AF1410 are essentially the same. As oxide particles found in these materials appear no more resistant to void nucleation than MnS particles, the oxides become the weak link in the fracture process.
7. The Ti_2CS particles in the experimental HY180 and AF1410 heats form as thin plates, having a broad range of sizes. The larger particles are sheets about 1-2 μm in extent and on fracture surface replicas these larger particles have shattered.
8. The Ti_2CS particles in the Ti_2CS heat of AF1410 did not dissolve until $1250^{\circ}C$. This suggests the particles are quite stable, will not dissolve at ordinary forging temperatures.

4.5.b Other conclusions

1. Blunting behavior is apparently insensitive to inclusion distributions and is determined by fine scale microstructure.
2. Blunting to vertices is associated with higher fracture toughness than smooth blunting provided the materials blunting to vertices and smooth blunting are characterized by the same plane strain tensile ductility and identical inclusion distributions.
3. Austenite grain size is not critical to toughness when the inclusions are large and widely spaced, but can be when the inclusions are small and closely spaced. This effect is quite strong when the sulfides are Ti_2CS .
4. Gettering sulfur as La_2O_2S rather than MnS improves the fracture toughness of HY180 steel and AF1410 steel for all three microstructures evaluated for these steels.

5. Students

This work was primarily that of Dr. J. Maloney who completed his Ph.D. thesis during the summer of 1992. Dr. Maloney is currently Head of Research at Latrobe Steel and Latrobe Steel contributed financially to the completion of this work.

6. Patents

A patent was applied for on getting sulfur as Ti_2CS prior to this three year period of work. However, the patent was awarded in March of 1992 with J. Maloney, J. Bray and W. Garrison as co-investigators.

7. Commercial Development

A specialty steel company is interested in pursuing commercial application of getting sulfur as Ti_2CS in four grades of ultra high strength steels which they produce.

8. References

1. J.L. Maloney and W. M. Garrison, Jr., *Scripta Metall.*, Vol. 23, 1989, 2097-2100.
2. K. J. Handerhan, W. M. Garrison, Jr. and N. R. Moody, *Metall. Trans.* Vol. 20A, 1989, 105-123.
3. ASTM E399-83, in Standard Test Method for Plane Strain Fracture Toughness of Metallic Materials, 1983 Annual Book of ASTM Standards, Section 3, American Society for Testing and Materials, Philadelphia, PA, 1983, 170.
4. J. F. Knott, in Fundamentals of Fracture Mechanics, Butterworths, London, 1973.
5. ASTM E813-81, in Standard Test Method for J_{IC}, a Measure of Fracture Toughness, 1983 Annual Book of ASTM Standards, Section 3, American Society for Testing and Materials, Philadelphia, PA, 1983, 762.
6. C. F. Shih, *J. Mech. Phys. Solids*, Vol. 29, 1981, 305.
7. J. Q. Clayton and J. K. Knott, *Metal Sci.*, Vol. 10, 1977, 290.
8. J. R. Rice and M. A. Johnson, in Inelastic Behavior of Solids, M. F. Kanninen, W. G. Adler, A. R. Rosenfield and R. I. Jaffee, eds., McGraw-Hill, New York, 1970, 641.
9. T. B. Cox and J. R. Low, *Metall. Trans.*, Vol 5, 1974, 1457.
10. J. L. Maloney, Ph.D. Thesis, Carnegie Mellon University, Pittsburgh, PA, 1992.
11. S. Eliot, private communication, Carnegie Mellon University, May, 1992.
12. G. R. Speich and W. A. Spitzig, *Metall. Trans.*, Vol. 13A, 1982, 2239.
13. K. J. Handerhan and W. M. Garrison, Jr., *Scripta Met.*, Vol. 22, 1988, 607-610.
14. K. J. Handerhan and W. M. Garrison, Jr., *Acta Metall. Mater.*, Vol. 40, 1992, 1337.
15. J. W. Bray, J. L. Maloney, K. S. Raghavan and W. M. Garrison, Jr., *Metall. Trans.*, Vol. 22A, 1991, 2277.
16. W. M. Garrison, Jr. and N. R. Moody, *Metall. Trans.*, Vol. 18A, 1987, 1257.
17. G. R. Speich, D. S. Dabkowski and L. F. Porter, *Metall. Trans.*, Vol. 4, 1973, 303.
18. F. A. McClintock, *J. Applied Mech.*, Trans. ASME Series H, Vol. 25, 1958, 363.
19. R. M. McMeeking, *J. Mech. Phys. Solids*, Vol. 25, 1977, 357.
20. R. M. McMeeking, *J. of Eng. Materials and Technology*, Trans. ASME, Series H, vol. 99, 1977, 290.
21. A. Wojcieszynski, W. M. Garrison, Jr. and A. W. Thompson, "The Influence of Grain Size on the Upper Shelf Toughness of a 9Ni Steel", *Scripta Metall.*, October, 1992.
22. A. Wojcieszynski, private communication, Carnegie Mellon University, Pittsburgh, PA, June, 1992.

Table 1
Primary Particle Characteristics,
 δ_{IC}/X_0 Ratio and Blunting Behaviors

Material	f	R_0 (μm)	X_0 (μm)	δ_{IC}/X_0	Blunting
Base	0.00036	0.28	3.49	2.69	-
Base+Ni	0.00039	0.26	3.15	3.49	-
Base+Si	0.00024	0.34	4.86	1.56	-
Base+Ni+Si	0.00027	0.68	9.33	2.35	-
Base+Ni+Si+MoV	0.00023	0.64	9.3	1.61	-
HP1 840-AQ	0.00022	0.25	3.7	2.78	Smooth
HP2 1050-AQ	0.00016	0.33	5.4	4.35	Smooth
HP2 1200-AQ	0.00017	0.44	7.4	5.9	Smooth
AF1410#1-425°C	0.00034	0.18	2.3	5.2	-
AF1410#1-510°C	0.00034	0.18	2.3	12.1	Vertices
AF1410#2-425°C	0.00042	0.64	7.6	3.0	-
AF1410#2-510°C	0.00042	0.64	7.6	8.68	Vertices
AF1410#3-425°C	0.00036	1.24	15.4	1.62	-
AF1410#3-510°C	0.00036	1.24	15.4	3.96	Vertices
HP2-AQ	0.00022	0.17	2.5	6.2	Smooth
HP2-200°C	0.00022	0.17	2.5	16.6	-
HP2-565°C	0.00022	0.17	2.5	37	Vertices
HP9-4-10-AQ	0.00036	0.19	2.4	18	Smooth
HP9-4-10-565°C	0.00036	0.19	2.4	65	Vertices
HY180-425°C	0.00042	0.18	2.14	24.3	Vertices
HY180-510°C	0.00042	0.18	2.14	40.65	Vertices

HP1 is the first heat of HP9-4-20 investigated and HP2 is the second.

Table 2
Compositions of Experimental Heats of HY180 Steel*

Heat	C	Ni	Co	Cr	Mo	Si	Mn	S	P	Ti	La	Nb	N ₂ **	O ₂ **
heat 1	.10	9.86	7.96	1.98	1.02	.01	.31	.002	.004	.004	<.002	.003	3	6
heat 2	.12	9.88	8.07	1.99	1.0	.01	.01	.001	.003	.003	.005	.003	3	8
heat 3	.11	9.88	8.07	1.99	1.00	.01	.01	.001	.003	.021	<.002	.003	1	4
heat 4	.11	9.90	8.02	1.99	1.01	.01	.01	.001	.003	.012	<.002	.003	1	12

* wt%

** wt ppm

Table 3
Inclusion Characteristics for Heats of HY180 Steel

Heat	Primary type	f	R ₀ (μm)	X ₀ (μm)
heat 1	MnS	0.00021	0.16	2.4
heat 2	La ₂ O ₂ S	0.00015	0.44	7.5
heat 3	Ti ₂ CS	0.00019	0.10	1.6
heat 4	Ti ₂ CS	0.00011	0.10	1.6

f = volume fraction; R₀ = average radius; X₀ = spacing

Table 4
Carbides Present After Austenitizing
and Grain Sizes for
Heats of HY180 Steel

Heat	Carbide type	f	2R ₀ (μm)	Linear Intercept Austenite Grain Size (μm)
heat 1	M ₂₃ C ₆ ,MC	0.0023	50	9.5
heat 2	M ₂₃ C ₆ ,MC	0.0019	53	10.5
heat 3	M ₂ C,MC	0.0048	18	7.1
heat 4	M ₂ C,MC	0.0017	13	7.0

TABLE 5
Summary of Mechanical Properties of HY180 Steel*

As-Quenched

Heat	YS (MPa)	UTS (MPa)	ϵ_f^{AX}	ϵ_f^{ps}	n	J_{IC} (MPa-m)	K_{IC} (MPa \sqrt{m})	δ_{IC} (μm)	C_v (J)
heat 1	1066	1431	1.15	0.31	0.10	0.17	181	68	117
heat 2	1037	1435	1.34	0.28	0.11	0.32	250	129	197
heat 3	1043	1428	1.43	0.30	0.11	0.41	286	165	214
heat 4	1065	1449	1.45	0.36	0.12	0.52	321	206	220

Tempered at 425°C

Heat	YS (MPa)	UTS (MPa)	ϵ_f^{AX}	ϵ_f^{ps}	n	J_{IC} (MPa-m)	K_{IC} (MPa \sqrt{m})	δ_{IC} (μm)	C_v (J)
heat 1	1170	1360	1.17	0.30	0.06	0.19	195	75	122
heat 2	1144	1348	1.30	0.31	0.06	0.26	227	104	131
heat 3	1195	1320	1.41	0.30	0.06	0.43	285	173	156
heat 4	1199	1391	1.41	0.33	0.06	0.42	287	175	153

Tempered at 510°C

Heat	YS (MPa)	UTS (MPa)	ϵ_f^{AX}	ϵ_f^{ps}	n	J_{IC} (MPa-m)	K_{IC} (MPa \sqrt{m})	δ_{IC} (μm)	C_v (J)
heat 1	1208	1343	1.39	0.36	0.043	0.33	267	129	174
heat 2	1236	1379	1.54	0.44	0.048	0.53	339	214	213
heat 3	1240	1369	1.58	0.37	0.044	1.06	480	406	267
heat 4	1260	1392	1.65	0.40	0.046	1.35**	550	509	290

* All K_{IC} and δ_{IC} values are calculated from J_{IC} .

** J_Q was 1.75; specimen dimensions were such J_Q would be J_{IC} if $J_{IC} = 1.35$ MPa-m

Table 6

**Materials and Heat Treatments Used to Test Effect
of Grain Size on Toughness at Two Particle Spacings**

Heat	C	Mn	Si	Ni	Cr	S	P	O ₂	N ₂
H1	.077	.37	.008	9.29	.26	20	.003	7	4
H2	.073	.23	<.01	9.08	.22	16	.004	5	2
H3+	.076	.01	<.01	9.44	.21	3	.003	18	12

* Given in weight %; S, O₂ and N₂ are in ppm by weight.

- H1 and H2 contain MnS
 - austenitize at low temperature to get fine grain size and small X₀
 - to get large grain size and small particle spacing, austenitize at high temperature to establish grain size and then quench to 790°C to reprecipitate MnS which dissolved at initial temperature, and then hold for 15 hrs and then quench to room temperature.

- H3 contains La₂O₂S
 - austenitize at low temperature to get fine grain size and large X₀.
 - can get large grain size at large X₀ by simply austenitizing at high temperature because La₂O₂S particles do not dissolve at high temperatures.

Table 7

**Inclusion Characteristics
and Austenite Grain Size
for 9Ni Steels**

Mat.	Heat Treat.	F_v	$R_0[\mu\text{m}]$	$X_0[\mu\text{m}]$	$I[\mu\text{m}]$
H1	790°C/WQ	.00027	.12	1.6	13.3
H1	1250/750/WQ	.00016	.11	1.9	151.0
H2	790°C/WQ	.00023	.095	1.4	13.5
H2	1250/750°C/WQ	.00015	.086	1.5	89.8
H3	790°C/WQ	.00026	.47	6.5	16.1
H3	1000°C/WQ	.00024	.46	6.6	163.2

F_v = inclusion volume fraction

R_0 = average inclusion radius

X_0 = average inclusion spacing

I = linear intercept grain size

Table 8
Compositions of Heats of AF1410 Steel*

Heat	C	Ni	Co	Cr	Mo	Si	Mn	S	P	Ti	La	Nb	N ₂ **	O ₂ *
heat A1 (MnS)	.17	9.88	13.90	2.06	1.10	.01	.28	.001	.002	.004	-	-	3	1
heat A2 (CrS)	.16	9.97	14.0	2.04	1.0	.01	.001	.001	.004	.003	-	-	9	10
heat A3 (La ₂ O ₂ S)	.16	10.10	14.04	2.10	1.00	.03	.03	.004	.004	.002	.006	-	3	9
heat A4 (Ti ₂ CS)	.16	9.98	14.10	2.01	1.01	.01	<.01	.001	.003	.013	-	-	2	7

* wt%

** wt ppm

Table 9
Inclusions in Heats of AF1410 Steel

Heat	Primary type	f	R ₀ (μm)	X ₀ (μm)
heat A1	MnS	0.00014	0.11	1.90
heat A2	CrS	0.00034	0.18	2.3
heat A3	La ₂ O ₂ S	0.00042	0.64	7.60
heat A4	Ti ₂ CS	0.00013	0.10	1.75

f = inclusion volume fraction

R₀ = mean inclusion radius

X₀ = mean spacing = 0.89 R₀f^{-1/3}

TABLE 10
Properties of Af1410 Heats Aged at 510°C

Heat	YS (MPa)	ϵ_f^a	n^b	J_{IC} (MPa-m)	K_{IC}^c (MPa \sqrt{m})	C_v^e (J)	$(\epsilon_f^{PS})^d$
MnS heat A1	1505	1.22	0.048	0.123	158	70	0.27
CrS heat A2	1527	1.16	0.06	0.075	128	61	0.24
La ₂ O ₂ S heat A3	1489	1.24	0.058	0.209	199	88	-
Ti ₂ CS heat A4	1483	1.39	-	0.53	341	205	-

- a) tensile ductility
- b) work hardening exponent
- c) K_{IC} calculated from J_{IC}
- d) plane strain ductility
- e) Charpy impact energy

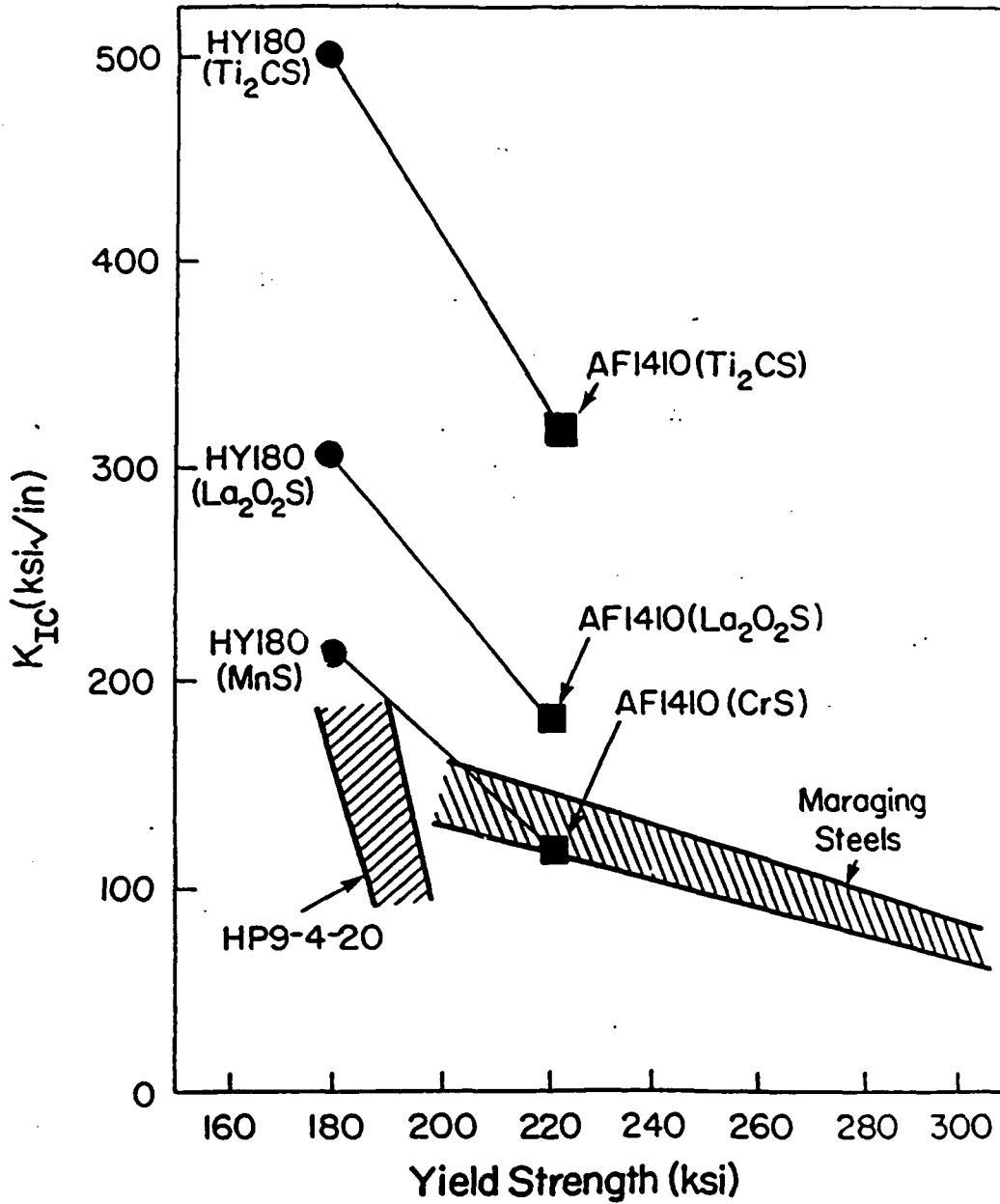
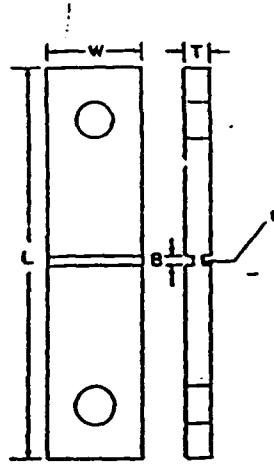


Fig. 1 Fracture toughness (K_{IC}) plotted as a function of yield strength. Data for HY180 and AF1410 steels containing MnS or CrS, $\text{La}_2\text{O}_2\text{S}$ or Ti_2CS are indicated. Data bands for HP9-4-20 and for maraging steels are included for comparisons.

Specimen



$$\epsilon_f = \ln(t_0/t_f)$$

Results of Speich and Spitzig

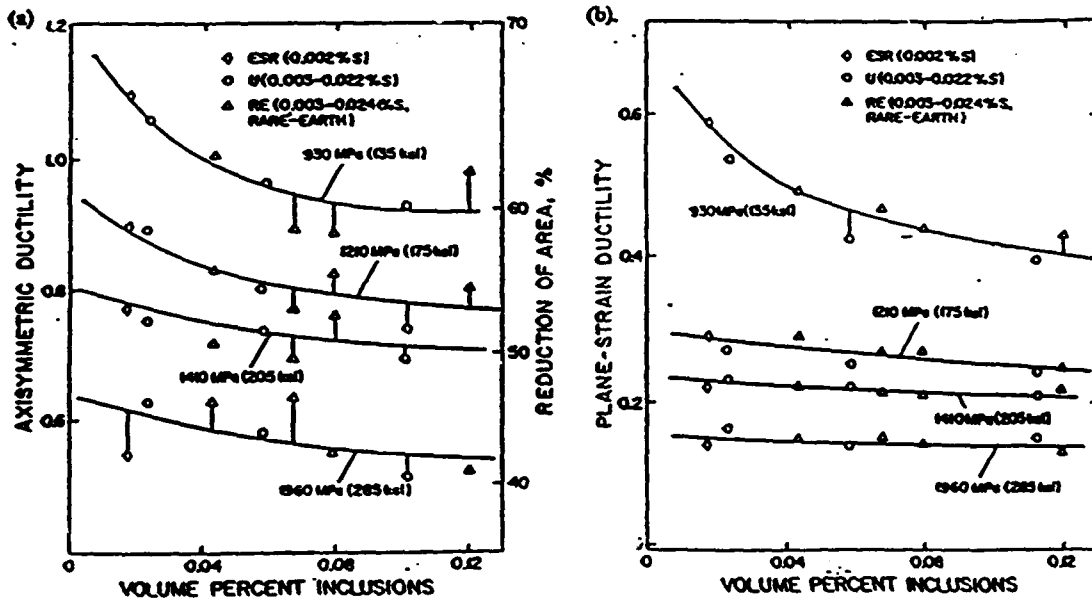


Fig. 24. (a) Axisymmetric and (b) plane strain tensile ductilities plotted as a function of inclusion volume fraction for 4340 steel tempered to the indicated strength levels [130].

Fig. 2 A schematic of the plane strain tensile specimen and the results of Speich and Spitzig for the (a) axisymmetric and (b) plane strain tensile ductility as a function of inclusion volume fraction for 4340 steel tempered to the indicated strength levels (Ref. 12).

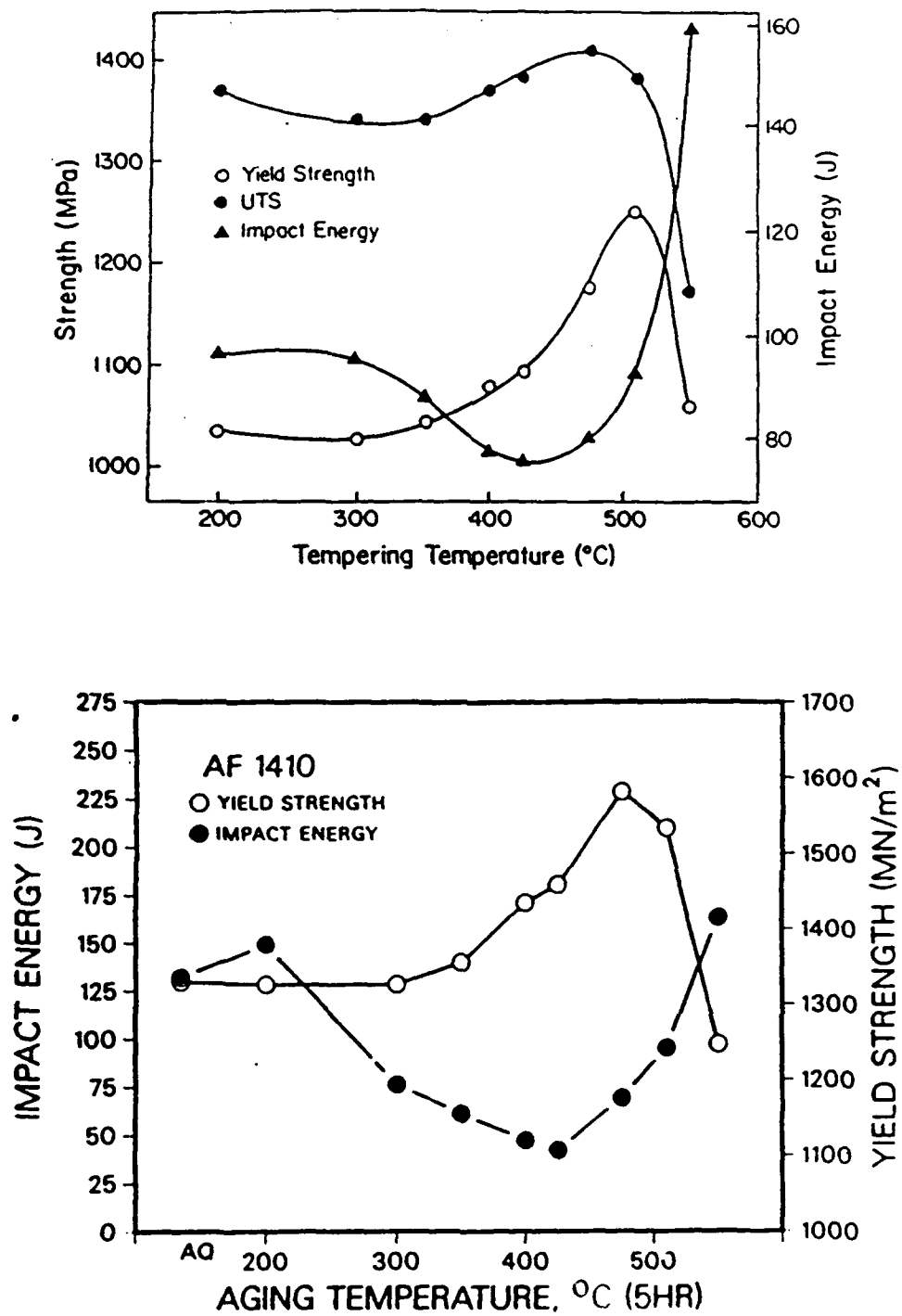


Fig. 3 Effect of tempering temperature on the strength and Charpy impact energy of (a) HY180 and (b) AF1410 steel.

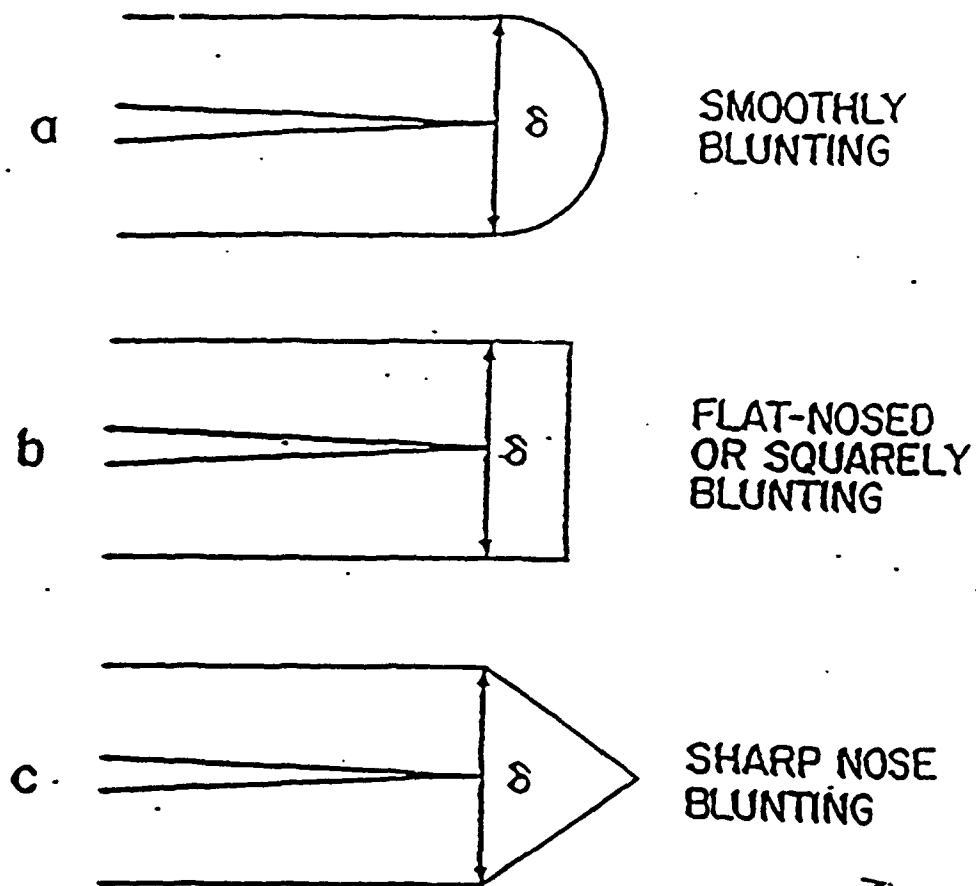


Fig. 4 Possible modes of blunting behavior suggested by McClintock (Ref. 18). In (a) the crack tip blunts smoothly and in (b) and (c) the crack tip blunts to 2 and 3 corners or vertices respectively.

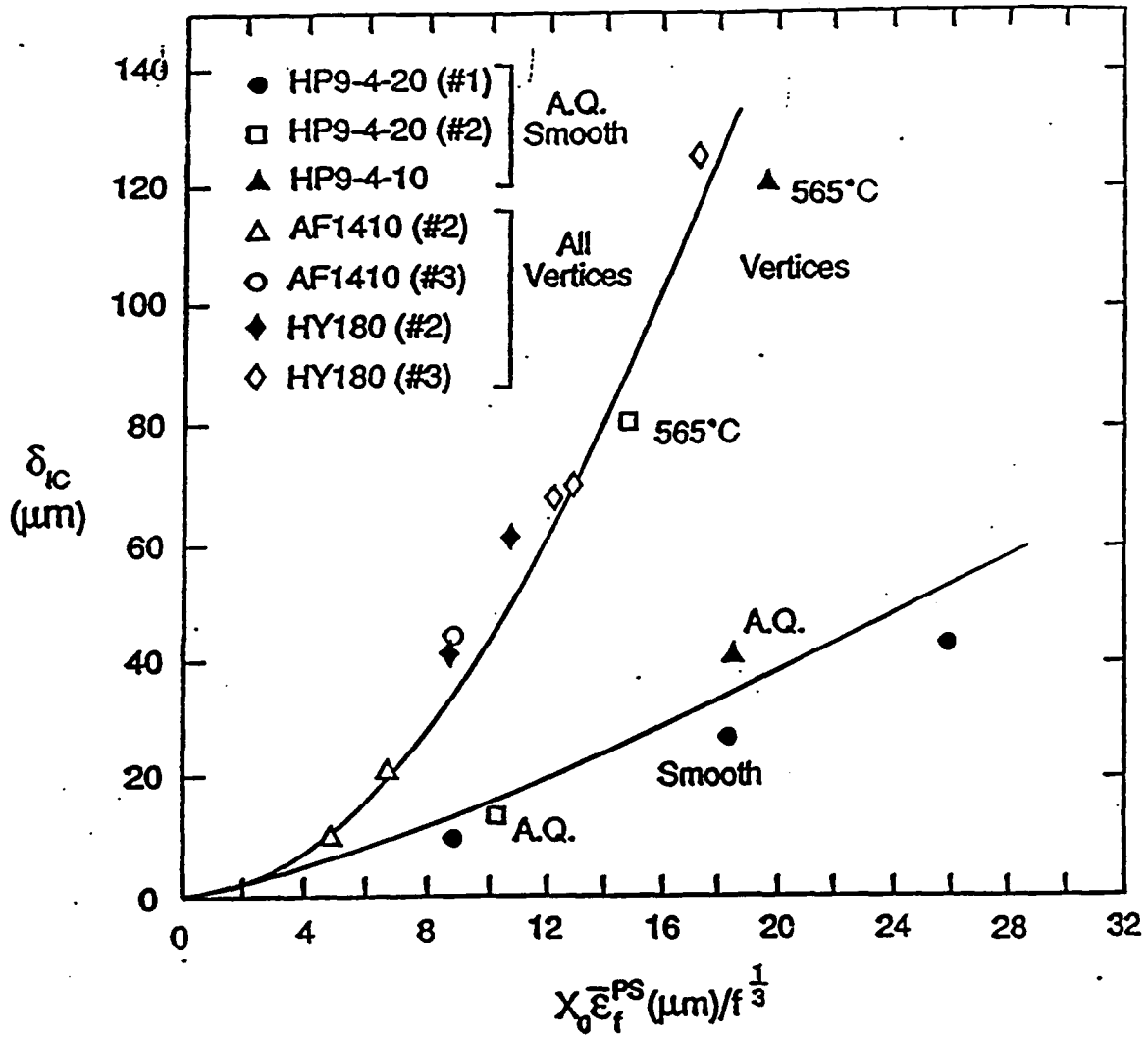
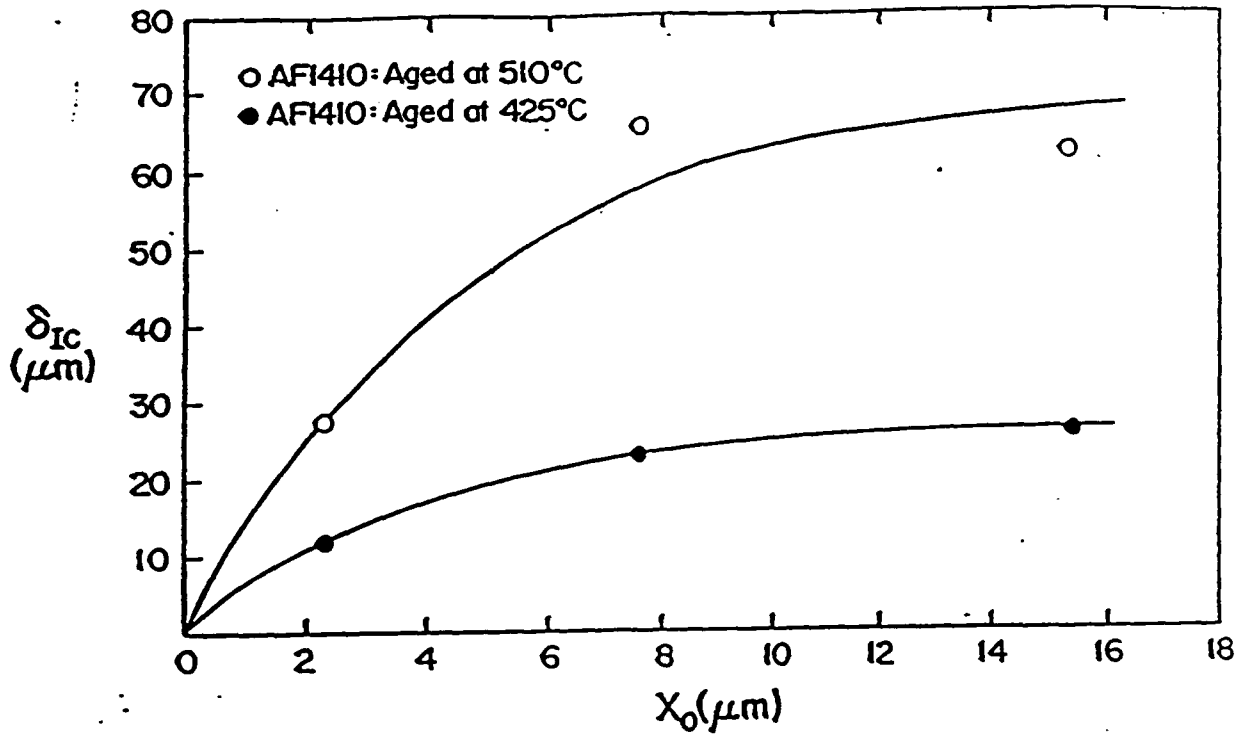


Fig. 5 δ_{IC} plotted as a function of $X_0 \bar{\epsilon}_f^{PS} / f^{1/3}$ for small X_0 . X_0 is the inclusion spacing, $\bar{\epsilon}_f^{PS}$ is the effective plane strain tensile fracture strain and f is the inclusion volume fraction.

δ_{IC} and X_0 at Constant f 

AF1410 steel	Type	f	R_0 (μm)	X_0 (μm)
heat 1 (no La add)	CrS	0.00036	0.19	2.4
heat 2	$\text{La}_2\text{O}_2\text{S}$	0.00042	0.64	7.5
heat 3	$\text{La}_2\text{O}_2\text{S}$	0.00036	1.24	15.4

Fig. 6 δ_{IC} plotted as a function of inclusion spacing, X_0 , at constant inclusion volume fraction for AF1410 steel tempered at 425°C or 510°C.

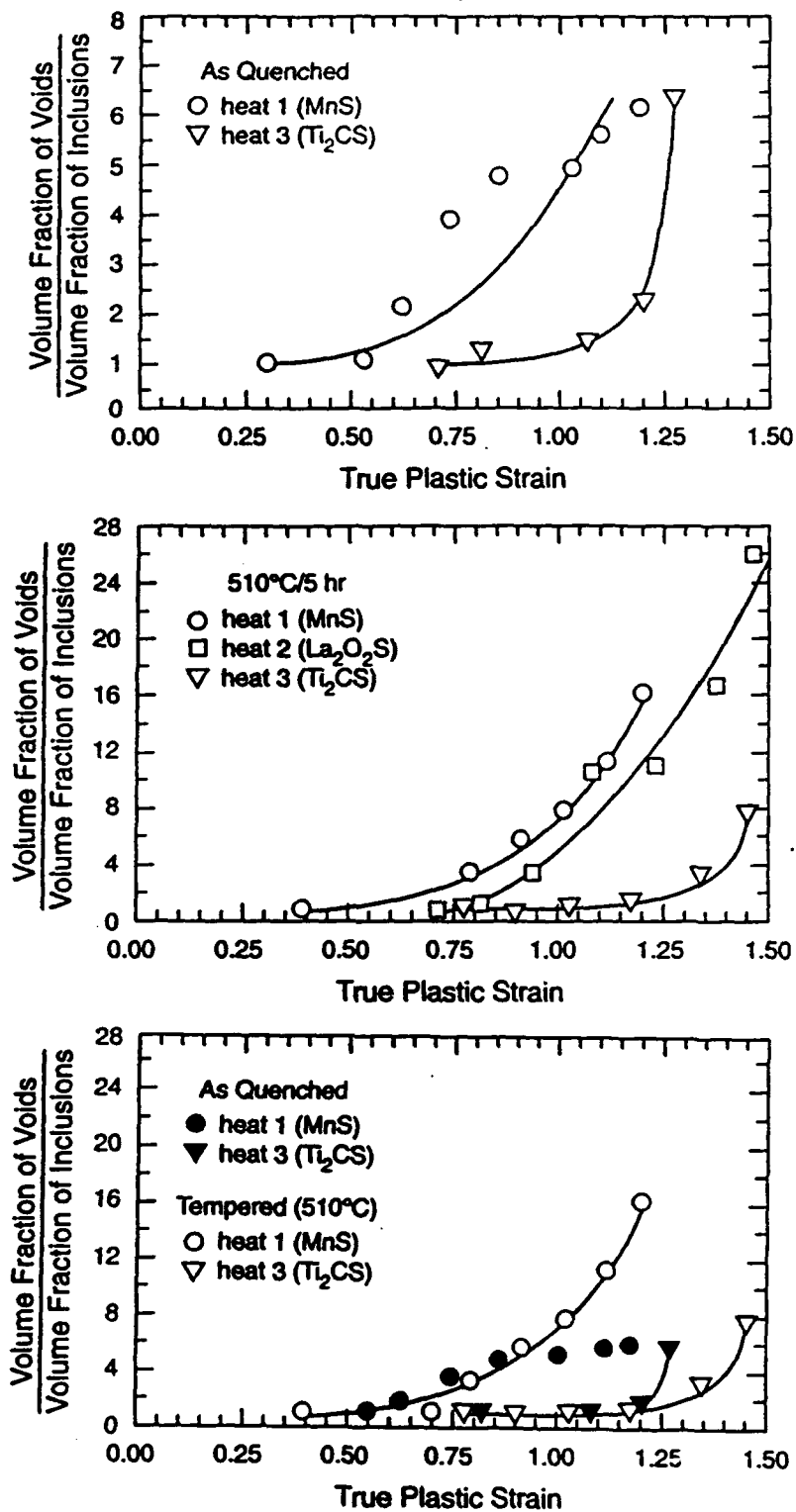


Fig. 7 Plots of void plus inclusion volume fraction normalized by inclusion volume fraction as a function of plastic strain in smooth axisymmetric tensile specimens. The results in (a) are for as-quenched HY180 and in (b) are for HY180 tempered at 510°C. In (c) results for the as-quenched and tempered at 510°C microstructures are compared.

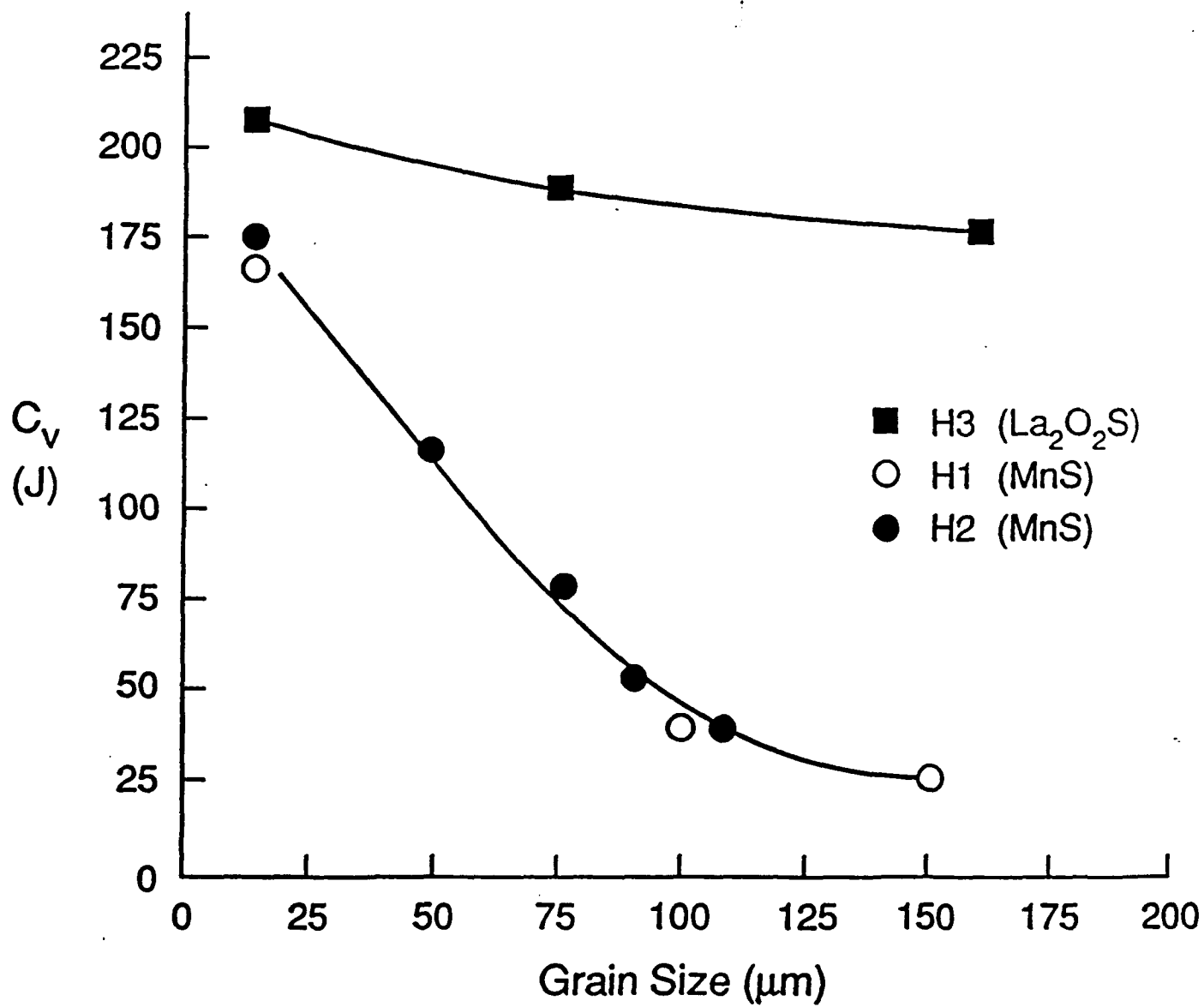


Fig. 8 Charpy impact energy as a function of austenite grain size for widely spaced ($\text{La}_2\text{O}_2\text{S}$) inclusions and closely spaced (MnS) inclusions.

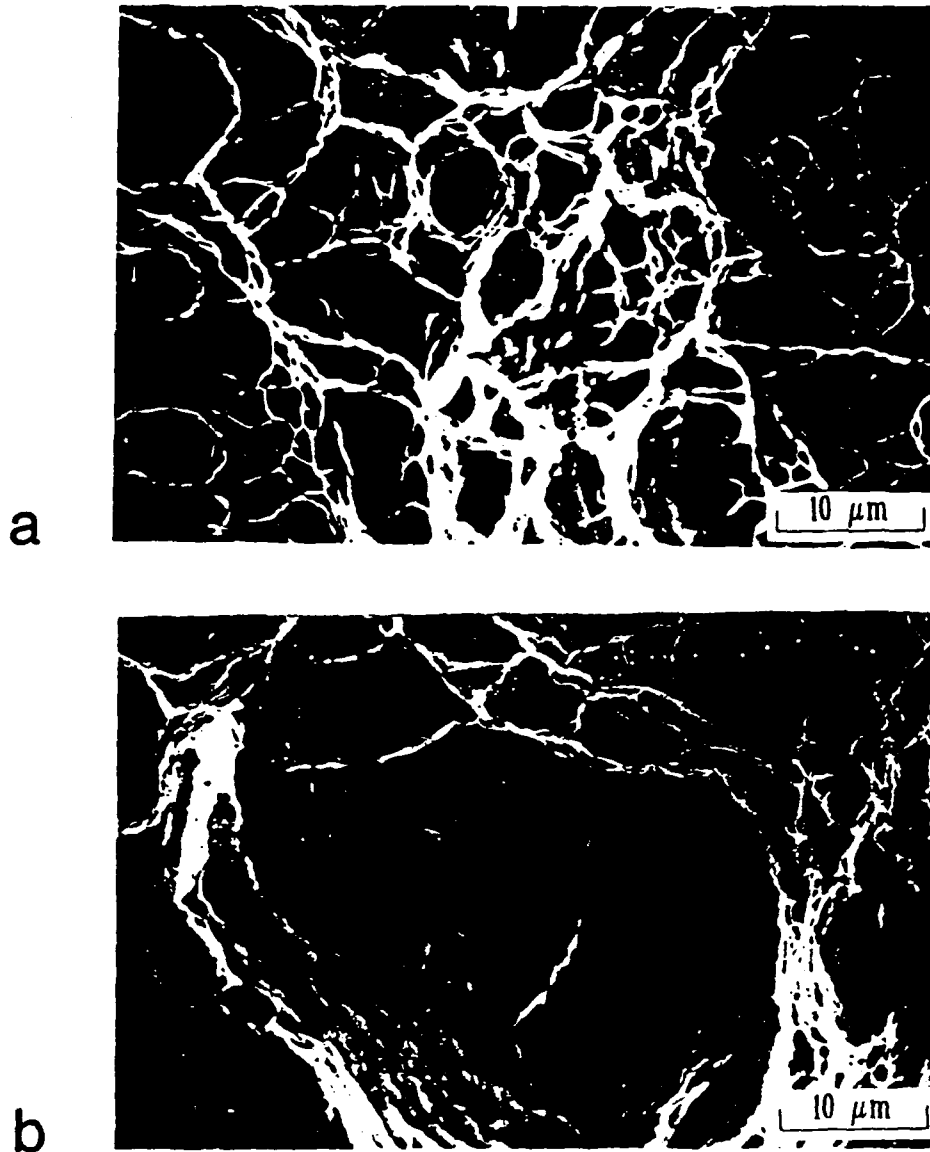


Fig. 9 Fracture surfaces of (a) HY180 heat 1 containing MnS and of (b) HY180 heat 3 containing Ti_2CS tempered at 510°C.

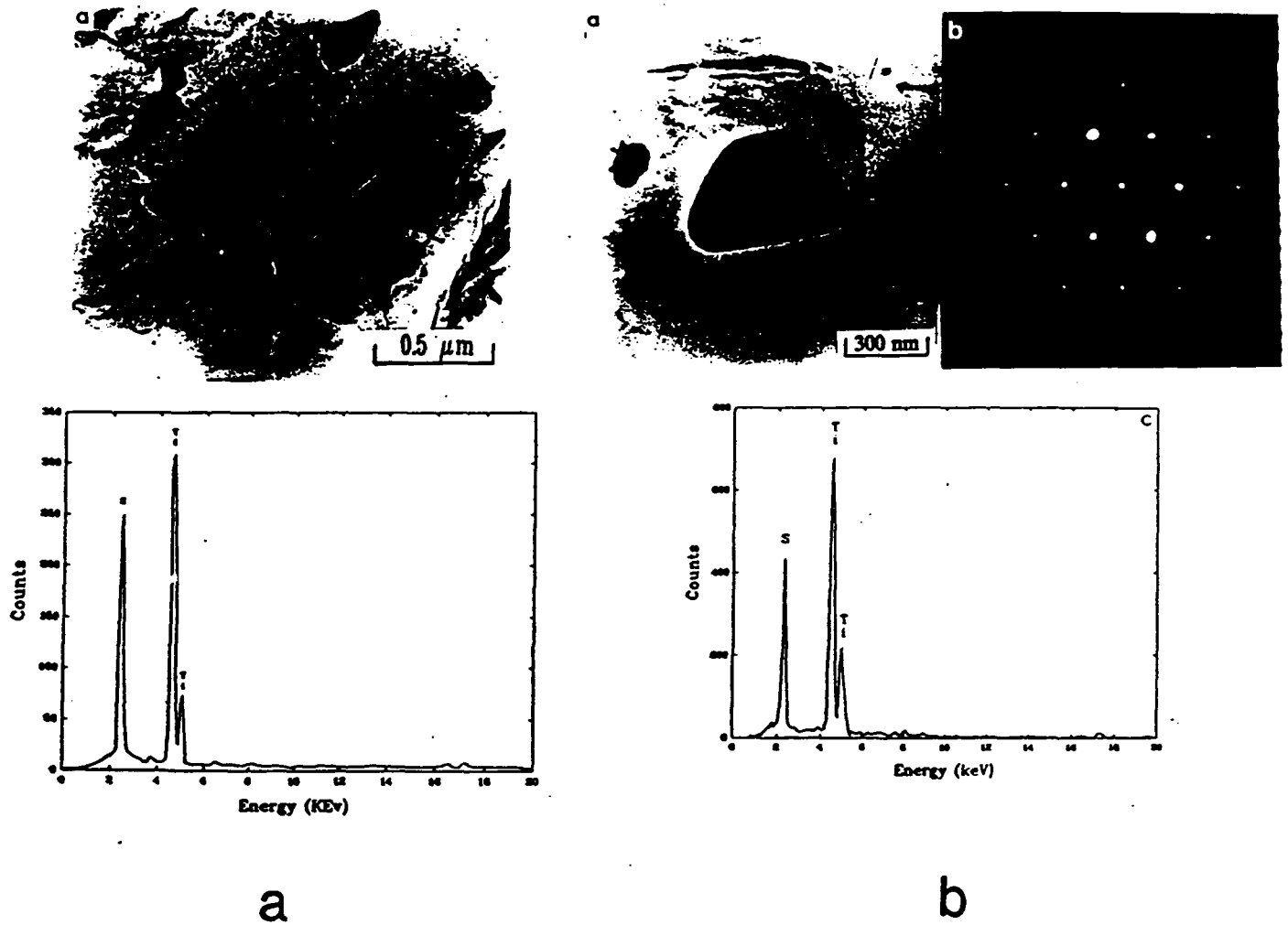


Fig.10 (a) Typical fractured Ti_2CS plate and its EDS spectrum.
 (b) Ti_2CS plate found in a dimple on a fracture surface of heat 3. (a) TEM bright-field, (b) [0001] HCP 3 zone axis SAD pattern. and (c) EDS spectrum of particle.